THE JOURNAL OF BIOLOGICAL CHEMISTRY VOL. 288, NO. 12, pp. 8391–8404, March 22, 2013

Identification and Cytoprotective Function of a Novel Nestin Isoform, Nes-S, in Dorsal Root Ganglia Neurons*[S]

Received for publication, August 14, 2012, and in revised form, January 2, 2013 Published, JBC Papers in Press, January 14, 2013, DOI 10.1074/jbc.M112.408179

Peng-Han Su[‡], Chih-Cheng Chen[§], Ya-Fan Chang[‡], Zong-Ruei Wong[‡], Kai-Wei Chang[‡], Bu-Miin Huang[¶], and Hsi-Yuan Yang[‡1]

From the [‡]Institute of Molecular and Cellular Biology, National Taiwan University, Taipei 10617, Taiwan, the [§]Institute of Biomedical Sciences, Academia Sinica, Taipei 115, and the [¶]Department of Cell Biology and Anatomy, National Cheng-Kung University, Tainan 701, Taiwan

Background: Nestin is a type VI intermediate filament protein widely used as neural stem cell marker.
Results: Nes-S, a novel nestin isoform that exerts cytoprotective functions, is identified in neurons of adult rats.
Conclusion: Nes-S may provide additional cytoprotection to support the long term survival of adult neurons.
Significance: This study reported the first nestin isoform, whose function may shed light on future studies of neurodegenerative diseases.

In this study, the first nestin isoform, Nes-S, was identified in neurons of dorsal root ganglia (DRG) of adult rats. Nes-S cannot form filaments by itself in cytoplasmic intermediate filament-free SW13 cells. Instead, it co-assembles into filaments with vimentin when transfected into vimentin$^+$ SW13 cells, and with peripherin and neurofilament proteins when transfected into N2a cells. In primary DRG neurons, endogenous Nes-S co-assembles with peripherin and neurofilament proteins. The expression of Nes-S first appears in DRG at postnatal day 5 and persists to adulthood. Among the adult tissues we examined, the expression of Nes-S is restricted to the sensory and motor neurons. Finally, exogenous Nes-S enhances viability when transfected into N2a cells, and knockdown of endogenous Nes-S impairs the survival of DRG neurons in primary cultures. Taken together, Nes-S is a new neuronal intermediate filament protein that exerts a cytoprotective function in mature sensory and motor neurons.

Nestin is a type VI intermediate filament (IF)[2] protein (1). It is also known as IFAP-70/280kD for hamster nestin and transitin for avian nestin (2–5). It is widely accepted that the IF cytoskeleton maintains the mechanical stability of most animal cells (6–8). This function is further enhanced by its cross-linking to actin filaments and microtubules, as well as to junctional complexes via intermediate filament-associated proteins (IFAPs), such as plectin/IFAP300 and the plakin family proteins (9–14). All of the IF proteins contain a central rod domain, which mediates coiled-coil dimer formation and leads to the assembly of the IFs. The rod domain is flanked at both ends with nonhelical sequences, the so-called N-terminal "head" and C-terminal "tail" domains, which are different in length and properties among IF proteins (15–18). Based on gene structure as well as nucleotide sequence homology of the region coding for the rod domain, the IF proteins are classified into six subtypes (5, 16, 19). Nestin and its homologue synemin (5, 20) comprise the type VI IF protein family, which is characterized by a distinct intron-exon pattern and a long C-terminal tail that often contains tandem repeat motifs (1, 5, 21). The rat nestin protein is 1893 amino acids (aa) in length, comprising a short 7-aa N-terminal head, a 307-aa rod domain, and a long, 1579-aa C-terminal tail that contains a 536-aa tandem repeat region (aa 641–1176) (1, 4, 22). The rat nestin gene consists of four exons and three introns, with the first two introns interrupting its rod domain in a manner similar to the three type IV neurofilament proteins. Thus, it has been proposed that nestin should be classified as a type IV IF protein (19). However, the presence of the distinct third intron within the C-terminal domain, as well as the low sequence homology between the rod domain of nestin and neurofilament proteins, favors its classification, together with synemin, as a distinct type VI IF protein family (1, 3, 5, 21, 22).

It is well known that nestin is mainly expressed in cells with high proliferating capacity, predominately in myogenic and neurogenic progenitor cells (for review, see Refs. 23 and 24). Enhancer elements that specifically regulate nestin expression in myogenic and neurogenic progenitor cells are located, respectively, in the first and second intron (25–27). In primarily cultivated rat aortic smooth muscle cells, nestin expression is induced by epidermal growth factor (EGF), thrombin, and platelet-derived growth factor (PDGF) (28, 29). During development of the nervous system, nestin is predominately expressed in neuronogenic and gliogenic progenitors. In central nervous system (CNS), the expression of nestin ceases in most mature neurons and astrocytes (1, 30, 31). In adult CNS, nestin can only be observed in neural progenitors at regions

* This work was funded by the National Science Council, Executive Yuan, Taiwan, through Grants NSC98-2320-B-002-034-MY2 (to H.-Y. Y.).
[S] This article contains supplemental Figs. S1–S14 and Tables S1 and S2.
[1] To whom correspondence should be addressed: Institute of Molecular and Cellular Biology, National Taiwan University, No. 1, Sec. 4, Roosevelt Rd., Taipei 10617, Taiwan. Tel.: 886-2-33662479; Fax: 886-2-33662478; E-mail: hyhy@ntu.edu.tw.
[2] The abbreviations used are: IF, intermediate filament; IFAP, intermediate filament-associated protein; Nes-S, Nestin short; DRG, dorsal root ganglia; NFH, neurofilament heavy polypeptide; IR, immunoreactivity; AChR, acetylcholine receptor; MTT, 3-(4,5-dimethylthiazol-2-yl)-2,5-diphenyltetrazolium bromide; EGFP, enhanced green fluorescent protein; tGFP, Turbo green fluorescent protein; TriG, trigeminal ganglia; SCG, superior cervical ganglia; aa, amino acid(s); nt, nucleotide(s); DIV, day *in vitro*; P, postnatal day; FL, full length.

undergoing active neurono- and gliogenesis, such as hippocampus and olfactory bulb, as well as a subset of neurons located in the basal forebrain (23, 30, 32). In rat peripheral nervous system, nestin expression ceases in differentiating neurons as soon as they express neurofilament proteins during early neurogenesis, but it is still expressed in satellite and Schwann cells of adult rats (23, 30). Notably, it is well known that nestin is re-expressed in the proliferating reactive astrocytes (33–35). However, the expression of nestin is rarely reported in adult neurons under both normal and injured conditions.

Nestin cannot form IFs by itself, but it can assemble into filaments with other IF proteins, such as vimentin and α-internexin (3, 36). The long C-terminal domain of nestin is proposed to protrude from the IF core, serving as cross-bridging spacers between IF bundles (3). Besides serving as a mechanical stabilizer, accumulating data have pointed to nonmechanical roles of nestin. Nestin may promote cell proliferation, presumably by facilitating the phosphorylation-dependent disassembly of vimentin IFs during mitosis (4, 37). In addition, it has been demonstrated that nestin regulates differentiation of skeletal myocytes (38, 39). Nestin facilitates Cdk5-dependent dispersion of acetylcholine receptor (AChR) clusters in neuromuscular junction of differentiating skeletal myocytes. The results also demonstrated that nestin enhances Cdk5 activity by acting as a scaffold for recruiting Cdk5 and its co-activator p35 (39). This finding is supported by a recent study showing that impaired motor coordination and excessive numbers of AChR clusters were observed in nestin-deficient mice (40). Notably, nestin has also been demonstrated to exert antiapoptotic functions in neuroblastoma ST15A cells and rat aortic smooth muscle cells under oxidative stress (41–43), as well as in podocytes under high glucose treatment (44).

For the last decade, many cytoplasmic IF genes, including keratins, vimentin, desmin, peripherin, glial fibrillary acid protein, and synemin, were reported to generate isoforms via alternative splicing or alternative translation (45–52). Furthermore, both transitin, the avian nestin ortholog, and the other type VI IF gene synemin generate multiple alternatively spliced products (46, 53). The expression of these isoforms is often tissue- and developmental stage-specific (54, 55). Thus, generation of IF isoforms is now considered as a new way to regulate IF organization and may be involved in the progression of neurodegenerative diseases (for review, see Ref. 24). In this study, we report the first isoform of nestin, Nes-S (for "nestin short," given the shorter length of this isoform), from DRG neurons of adult rats. As compared with nestin, Nes-S lacks a large portion of the C-terminal domain, including the whole tandem repeat motifs. This alternative splicing introduces a frameshift mutation and a premature stop codon in the Nes-S tail region, leading to the translation of a 45.9-kDa protein. The expression of Nes-S in DRG first appeared at the postnatal day 5 (P5). Among the adult tissues we examined, the expression of Nes-S is restricted to the sensory and motor neurons. Nes-S cannot form filaments by itself, but can co-assemble with vimentin or neurofilament/peripherin proteins into IFs. Furthermore, Nes-S exerts a cytoprotective function when transfected into N2a cells, and knockdown of endogenous Nes-S impaired the survival of primary DRG neurons during prolonged cultures. These results indicate that Nes-S may play a role in the survival of sensory and motor neurons of adult rats.

EXPERIMENTAL PROCEDURES

Materials—All reagents were purchased from Sigma-Aldrich if not specified otherwise.

Sequences—The nucleotide numbers of the primers, probes, and regions of nestin transcript sequences correspond to the cDNA sequence of rat nestin (National Center for Biotechnology Information (NCBI) accession number AF538924.1). The amino acid numbers correspond to the sequence of 1893-aa rat nestin protein (NCBI accession number AAN33053.1).

Animals—Rats were purchased from BioLASCO (Taipei, Taiwan). Adult male Sprague-Dawley rats of 6–8 weeks old were used for the identification and tissue distribution studies of Nes-S. Pregnant Sprague-Dawley rats of known gravid stage were purchased, and the day of birth was designated as P0. For developmental studies, rats of embryonic day 12, P0, P1, P2, P5, P8, as well as adult rats, were used. The animals were sacrificed under anesthesia with an intraperitoneal administration of sodium pentobarbital (30 mg/kg of body weight). These procedures were approved by the Institutional Animal Care and Use Committees of National Taiwan University.

Northern Blotting—The Northern blotting experiments were performed with the digoxigenin labeling and detection system (Roche Applied Science) following the manufacturer's instructions. The bands of ribosomal 18 S and 28 S RNA were marked as molecular markers of 1.9 and 5 kb, respectively. The signals were developed by nitro blue tetrazolium/5-bromo-4-chloro-3-indolyl phosphate reagents (Promega). Details regarding the synthesis procedures and sequences of the probes are listed in the supplemental Methods.

In Situ Hybridization—For *in situ* hybridization, lumbar 4 or lumbar 5 DRG of adult rats was fixed in 4% paraformaldehyde dissolved in phosphate-buffered saline (PBS) at 4 °C for 24 h. The fixed DRG specimens were dehydrated, embedded in paraffin, sectioned, and then mounted on silane-coated microscope slides (Muto-Glass). To perform hybridization, the sections were deparaffinized, rehydrated, treated with protease K (2.5 mg/ml) for 5 min at 37 °C, and then post-fixed with 4% paraformaldehyde in PBS for 10 min at room temperature. The *in situ* hybridization was performed with the digoxigenin labeling and detection system (Roche Applied Science) following the manufacturer's instructions. Details regarding the probe sequences and probe synthesis procedures are listed in the supplemental Methods.

Antibodies—The antibodies used in the current study are listed in supplemental Table S1. The Nes-S-specific rabbit polyclonal antibody anti-AY14 was prepared by GenScript Inc.

Immunofluorescence Microscopy—Double or triple labeling immunofluorescence microscopy of tissue and cell samples, as well as double labeling of two primary mouse monoclonal antibodies using the Zenon mouse immunoglobulin G (IgG) labeling kit (Invitrogen), was performed as described with a few modifications (28, 56). The details regarding the staining procedures, as well as the parameters of confocal microscopy, including pinhole settings, laser lines, and objective lenses, are listed in the supplemental Methods.

Single Neuron RT-PCR—Primary cultures of adult DRG neurons were prepared as described previously with a few modifications (57). After dissociation, neurons were cultured for 6 h and then collected by glass micropipettes under an inverted fluorescence microscope with the aid of Hoechst 33342 (Invitrogen) live cell nuclear staining (supplemental Fig. S1, *D* and *E*). The total RNA content was purified with an Absolutely RNA nanoprep kit (Stratagene). Reverse transcription was carried out with RevertAid premium reverse transcriptase (Fermentas) following the manufacturer's instructions. PCR was performed with TaqDNA polymerase master mix Red (Ampliqon). Primer sequences and the details of PCR program settings are described in the supplemental Methods.

Plasmids and Cloning—Primer sequences and the cloning procedures are described in the supplemental Methods.

Cell Culture and Transfection—C6 glioma cells, HEK293T cells, SW13 cells, and N2a neuroblastoma cells were cultured in Dulbecco's modified Eagle's medium (DMEM) supplied with 10% FBS and 1% penicillin/streptomycin (Invitrogen) in a 37 °C humidified incubator supplied with 5% CO_2. Transfection of HEK293T, SW13, and N2a cells was performed by electroporation according to the manufacturer's instructions (Nucleofector, Amaxa Biosystems). To generate stable clones, N2a cells were transfected with pEGFP, pEGFP-NestS, pEGFP-NestS-T316A, or pEGFP-NestS-T316D, cultured for 2 days, and selected with a G418-containing medium (800 μg/ml) for 2 weeks. Single G418-resistent N2a clones were then isolated by limited dilutions.

Intermediate Filament-enriched Preparations, Whole Cell Extractions, and Immunoblotting Analysis—IF-enriched preparations of the rat tissues, whole cell extractions of HEK293T and N2a cells, and immunoblotting analysis were carried out as described previously with the following modification (28). The denatured protein samples were separated by 5–15% linear gradient SDS-polyacrylamide gel electrophoresis and processed for immunoblotting assay.

Immunoprecipitation—Immunoprecipitation assay was performed as described (42) with the following modifications. Whole cell lysates were incubated for 4 h with 2.5 μl of anti-GFP antibody followed by adding 25 μl of protein A/G-agarose beads (Santa Cruz Biotechnology) for another 16 h at 4 °C. The immunoprecipitated complexes were then assayed by immunoblotting with anti-Cdk5 antibody.

MTT Assay—MTT assay was performed as described with the following modifications (42). For proliferation assay, N2a cells were seeded at a density of 1000 cells/well into 96-well plates. For cell viability assay, N2a cells were seeded at a density of 1×10^4 cells/well into 96-well plates.

Nes-S RNAi in Primary DRG Neuron Culture—An shRNA sequence (5′-CAAGATGTCCCTTAGTCTGGAGGTGGCTA-3′) targeting the rod domain of rat nestin was synthesized and cloned into the pGFP-V-RS shRNA expression vector (OriGene Technologies). To knock down Nes-S in DRG neurons of adult rats, $\sim 1 \times 10^5$ of freshly dissociated neurons were suspended in 100 μl of BTXpress electroporation buffer (Harvard Apparatus) containing 50 μg of nestin shRNA plasmid, loaded into a 2-mm gap cuvette, electroporated with a BTX ECM 830 pulse generator with a single 15-ms pulse of 125 V (Harvard Apparatus), plated immediately on poly-lysine/laminin-coated coverslips, and cultured in F12-FBS medium and 100 ng/ml 7 S nerve growth factor (NGF). For control, DRG neurons were transfected with the nonfunctioning shRNA vector (OriGene, TR30008) by the same procedure. At the second day, the coverslips were incubated with fresh medium containing 1 μM 1-β-D-arabinofuranosyl cytidine to inhibit proliferation of the glial cells during the prolonged experiment period. The medium was changed daily to supply fresh NGF and 1-β-D-arabinofuranosyl cytidine during the course of the experiment. Transfected neurons were imaged by the DeltaVision live cell imaging system (Applied Precision).

RESULTS

In Situ Hybridization Evidence for a Nestin Transcript Variant in Adult DRG Neurons—In adult DRG, nestin was only observed in satellite and Schwann cells (30, 58). To ascertain this, triple labeling immunofluorescence microscopy of DRG tissue sections of adult rats with the mouse monoclonal Rat-401 anti-nestin antibody, as well as mouse monoclonal anti-neurofilament heavy polypeptide (NFH) and goat polyclonal anti-peripherin, was performed because the sum of NFH^+ and $peripherin^+$ neurons represents the whole population of DRG neurons (59). Consistent with previous studies (30, 58), the results revealed that although Rat-401 recognized satellite cells and Schwann cells, it did not label any of the DRG neurons (Fig. 1, *A–D*). The same result was also observed in primary cultures of adult DRG neurons (supplemental Fig. S1, *A–D*). However, *in situ* hybridization of DRG tissue sections with an antisense probe specific only to the 3′ end of rat nestin mRNA coding region (*Tail*, nt 5178–5682, Fig. 1*E*), as revealed by NCBI nucleotide BLAST search, showed that specific signals were detected in all of the DRG neurons in addition to satellite and Schwann cells (Fig. 1, *F* and *G*). Taken together, these results indicated that adult DRG neurons express nestin isoforms that do not contain the epitope of Rat-401.

Epitope Mapping of the Rat-401 Antibody—The epitope of Rat-401 remains unknown (1, 30). To prepare appropriate primers for isoform identification by RT-PCR, epitope mapping of Rat-401 was performed. Nestin cDNA was divided into five overlapping fragments, and each fragment was cloned into the expression vector pEGFP-C and expressed in HEK293T cells (supplemental Fig. S2*A*). The expressed peptides were analyzed by immunoblotting, and the results revealed that Rat-401 specifically recognized the peptide containing the tandem repeat region (supplemental Fig. S2*B*). This result also indicated that the nestin isoforms in mature DRG neurons do not contain the repeat region.

A Novel Nestin Splice Variant Identified by Single Neuron RT-PCR—Primary cultures of adult rat DRG were used to identify the nestin splice variant. To avoid contamination from the $Rat\text{-}401^+$ glial cells, which is predominant in DRG cultures, single DRG neurons were collected (supplemental Fig. S1, *E–H*), and the total RNA content of 10 neurons was isolated and subjected to RT-PCR. We first examined the C-terminal domain of nestin with the primer set that contains exon3F (nt 932–951) and exon4TailR (nt 5414–5433) (supplemental Fig. S3*A*). For control, RT-PCR on C6 glioma cells, which express

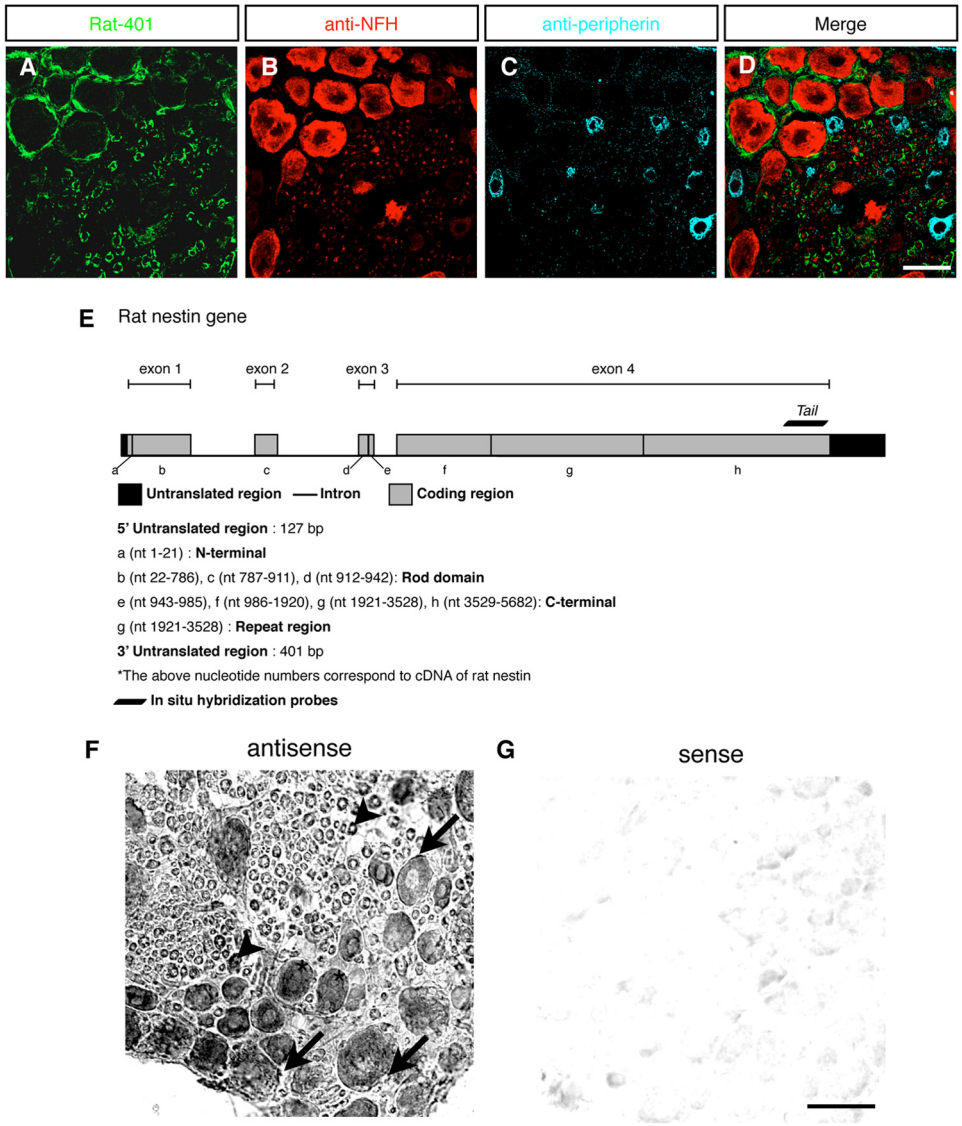

FIGURE 1. **The nestin transcript variant in DRG neurons of adult rats.** *A–D*, triple labeling of DRG sections of adult rats with Rat-401 (*A*), anti-NFH (*B*), and anti-peripherin (*C*). Although satellite cells and Schwann cells were Rat-401$^+$, all of the DRG neurons were Rat-401$^-$. *D* shows merged images. *E*, schematic diagram of the gene structure of rat nestin and the location of the *in situ* probe *Tail* (nt 5178–5682). The coding regions of rat nestin gene were designated as regions from *a* to *h*. *F* and *G*, *in situ* hybridization of DRG sections of adult rats with the antisense probe *Tail*. Specific signals were identified in neurons, satellite cells (*arrows*), and cytoplasm of Schwann cells surrounding the neuronal processes (*arrowheads*) (*F*). The sense probe of *Tail* was used as the negative control (*G*). *Scale bar*: 50 μm.

the full-length nestin (nestin-FL) (4), was performed. The RT-PCR results showed that although a 4.5-kb band was amplified in C6, a distinct 0.5-kb major band was produced in DRG neuron RNA (supplemental Fig. S3*B*). To amplify and to verify the specificity of this 0.5-kb band, semi-nested PCR was performed using the primer set exon3F (nt 932–951)-exon4TailiR (nt 5367–5388) on 10-fold serial dilutions of the first PCR product. The 0.5-kb band was successfully amplified in the second PCR (supplemental Fig. S3*C*). Cloning and sequencing results revealed that this band is 430 bp in length and corresponds to an alternatively spliced variant, in which a 4027-bp-long region of the exon 4 of nestin, including the coding sequence for the repeat region, was removed. The deletion junction contains a donor site-like splice cassette (TCAGG) at nt 1125 and an acceptor site-like splice cassette (TCAGG) at nt 5152 (supplemental Fig. S3*D*). On the other hand, cloning and sequencing of the 4.5-kb band obtained from the first RT-PCR of C6 cells revealed that it corresponds to the nestin-FL sequence from nt 932 to nt 5433.

Next, we examined the 5′ region of nestin (nt 1–1009), which includes the N-terminal domain (nt 1–21), rod domain (nt 22–942), and a part of the C-terminal domain (nt 943–1009). RT-PCR on DRG neuron RNA was performed with the second primer set that contains exon1F (nt 1–21) and exon4R (nt 989–1009) (supplemental Fig. S3*E*). C6 glioma RNA was used for control. The results showed that an 1-kb band was produced in both DRG neuron and C6 glioma RNA (supplemental Fig. S3*F*). Both RT-PCR products were subjected to the semi-nested PCR procedure using the primer set exon1F (nt 1–21)-exon3R (nt 963–982). The sequencing results revealed that both bands correspond to the known nestin-FL cDNA sequence (supplemental Fig. S3*G*). Because no in-frame translational start codon was

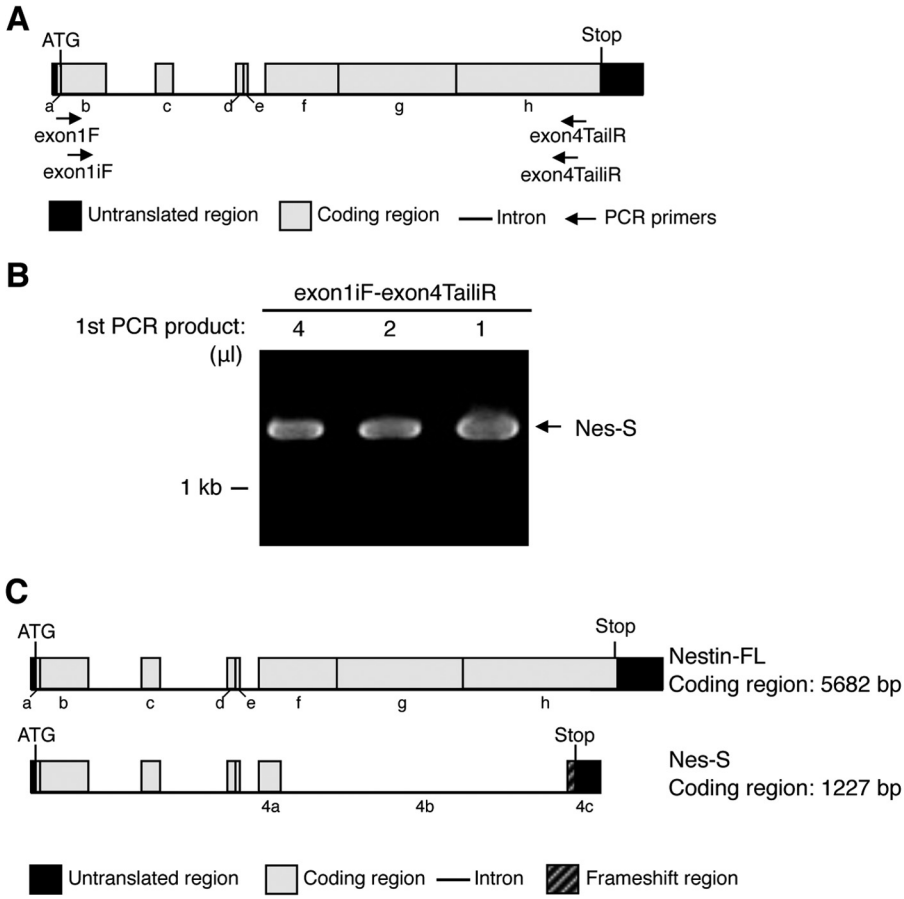

FIGURE 2. **Identification of the Nes-S transcript variant in DRG neurons by RT-PCR.** *A*, schematic diagram showing locations of the primers used to identify the complete cDNA of Nes-S. The coding regions of rat nestin gene were designated as regions from *a* to *h*. *B*, nested RT-PCR of DRG neuron RNA. The nested RT-PCR was performed using the primer set exon1F-exon4TailR and followed with the primer set exon1iF-exon4TailiR. A specific 1.3-kb band was produced. *C*, *upper panel*, schematic diagram of the nestin-FL. *Lower panel*, schematic diagram of the splicing pattern of the 1.3-kb band, which was named as Nes-S.

found within the 5′-untranslated region of the rat nestin gene, as revealed by genomic sequence analysis, the longest open reading frame of this transcript variant begins with the same start codon of the full-length rat nestin.

To amplify the full sequence of this nestin transcript variant, we performed RT-PCR on DRG neuron RNA using the primer set exon1F-exon4TailR followed by nested PCR procedure using the primer set exon1iF-exon4TailiR (Fig. 2*A*). The results showed that an 1.3-kb band was produced (Fig. 2*B*). Cloning and sequencing revealed that it corresponds to the cDNA sequence of the transcript variant. Given the shorter length of this isoform, we named this nestin isoform nestin short (Nes-S). Its complete coding region is 1227 bp in length. The mRNA of Nes-S is produced by splicing all three canonical introns and skipping the 4027-bp-long region (nt 1125–5151), which includes the whole repeat region (nt 1921–3528), in nestin exon 4 (Fig. 2*C*). We differentiated nestin exon 4 into three portions, including the 4027-bp-long alternative intron as exon 4b, and the regions upstream and downstream as exon 4a and exon 4c, respectively (Fig. 2*C*). Because this junction changes the translational open reading frame and results in a premature stop codon, a novel 32-aa domain was produced in the end of the tail region (Fig. 2*C*, also see supplemental Fig. S4). The length of Nes-S protein is 408 aa long, containing a 7-aa N-terminal domain, a 307-aa rod domain, and a 94-aa C-terminal tail region, with a predicted molecular mass of 45.9 kDa (Fig. 2*C*, also see supplemental Fig. S4).

Confirmation of the Existence of Nes-S mRNA by Northern Blotting and in Situ Hybridization—To confirm the existence of Nes-S mRNA, a Northern blotting experiment was performed on total RNA isolated from whole DRG tissues. The mRNA of Nes-S should be 1919 bp in length, including the 5′- and 3′-untranslated regions (supplemental Fig. S5*A*). As expected, the results revealed that, when hybridized with the probe *Tail*, two bands corresponding to the mRNA of the 5.9-kb nestin-FL and the 1.9-kb Nes-S were generated, respectively (supplemental Fig. S5*B*, *right*). On the other hand, when hybridized with the probe targeting to the spliced exon 4b (*E4b*, nt 3853–4792), only the 5.9-kb band of nestin-FL was detected (supplemental Fig. S5*B*, *left*).

Earlier results of *in situ* hybridization with the probe *Tail* (Fig. 1, *F* and *G*) revealed the existence of Nes-S mRNA in DRG neurons. To further confirm the expression of Nes-S mRNA in DRG neurons, *in situ* hybridization of DRG sections was performed with two additional antisense probes, *i.e.* the probe *Rod* (nt 321–762) located within the rod domain of Nes-S mRNA and the probe *E4b* (supplemental Fig. S5*A*). The results showed that, consistent with the probe *Tail*, the probe *Rod* labeled all of the DRG neurons, as well as satellite and Schwann cells (supplemental Fig. S5, *C* and *D*). On the other hand, the probe *E4b*

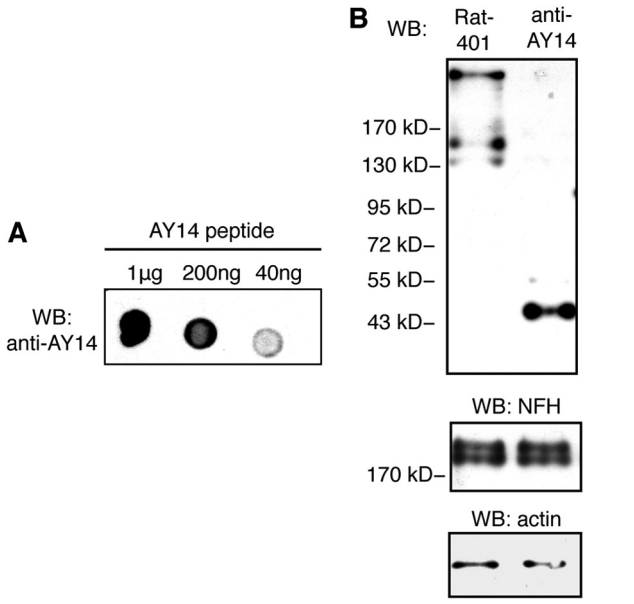

FIGURE 3. **Identification of Nes-S protein by immunoblotting of IF-enriched preparations of DRG with anti-AY14.** *A*, dot blotting of the synthesized AY14 peptide with anti-AY14. The specificity of anti-AY14 was confirmed. *WB*, Western blotting. *B*, immunoblotting of IF-enriched preparations of DRG of adult rats with Rat-401 and anti-AY14. Although Rat-401 recognized the band corresponding to nestin-FL, anti-AY14 specifically recognized the 45.9-kDa band of Nes-S protein. Immunoblotting with anti-actin and immunoblotting with anti-NFH were used as loading controls.

failed to recognize any DRG neurons and only labeled the satellite and Schwann cells (supplemental Fig. S5, *E* and *F*).

Identification of Endogenous Nes-S Protein by an Isoform-specific Antibody—NCBI protein BLAST search indicated that the 32-aa frameshift region of Nes-S tail is a novel sequence. A 14-aa peptide (AY14, AARSRILPKEETRY, also see supplemental Fig. S4) within this region was synthesized, and an isoform-specific rabbit polyclonal antibody, anti-AY14, was generated accordingly. This antibody was affinity-purified by immunoaffinity chromatography using the AY14 peptide, and its specificity was confirmed by dot blotting analysis against the AY14 peptide (Fig. 3*A*).

To further confirm the specificity of anti-AY14 and to verify the expression of the endogenous Nes-S protein in DRG of adult rats, an immunoblotting assay of IF-enriched preparation samples of DRG was carried out. The results showed that although Rat-401 recognized nestin-FL, anti-AY14 specifically recognized a distinct band around 45.9 kDa, which is consistent with the predicted molecular mass of Nes-S (Fig. 3*B*). In addition, immunofluorescence microscopy of C6 glioma cells, N2a neuroblastoma cells, HEK293T cells, and rat aortic smooth muscle cells with anti-AY14 showed that no specific signals were detected (supplemental Fig. S6), indicating that anti-AY14 did not cross-react with other cytoplasmic IFs, including vimentin, glial fibrillary acid protein, peripherin, keratin, and desmin.

Expression of Nes-S in DRG Neurons of Adult Rats—The expression of Nes-S was examined in DRG tissue sections of adult rats by double labeling with anti-AY14 and Rat-401. The results showed that anti-AY14-IR was specifically found in DRG neurons, but not in the Rat-401$^+$ satellite and Schwann cells (supplemental Fig. S7, *A–C*). When DRG tissue sections were triple-labeled with anti-AY14, anti-NFH, and anti-peripherin, anti-AY14-IR was observed in all of the DRG neurons (Fig. 4, *A–D*, also see supplemental Fig. S8, *A–H*). Weak anti-AY14-IR was also observed in the axoplasm of the peripheral processes of DRG, ventral roots of spinal cord, and sciatic nerves (supplemental Fig. S7, *G–J*). To examine the expression of Nes-S in adult DRG neurons, primary cultures of DRG were double-labeled with anti-AY14 and Rat-401. The results showed that anti-AY14-IR was specifically observed in many Rat-401$^-$ cells, but not in the Rat-401$^+$ glial cells (supplemental Fig. S7, *D–F*). To further confirm the neuronal expression of Nes-S, primary DRG cultures were triple-labeled with anti-AY14, anti-NFH, and anti-peripherin. The results showed that both NFH-IR and peripherin-IR were present in all of the cultivated DRG neurons (Fig. 4, *F* and *G*), and anti-AY14-IR was observed in all of these DRG neurons (Fig. 4, *E–H*). It is of interest to note that high magnification confocal microscopy showed that the IFs formed a cage-like cytostructure at the periphery of neurons and extended into the neurites. Enriched anti-AY14-IR was observed at the tip regions of these neurites (Fig. 4, *I–L*, also see supplemental Fig. S8, *I–X*).

Filament Assembly Properties of Nes-S—To further investigate the filament assembly properties of Nes-S, SW13 cells were transfected with pEGFP-NestS, a plasmid expressing Nes-S N-terminally labeled with enhanced green fluorescent protein (EGFP). It is known that the majority of SW13 cells do not express any cytoplasmic IF proteins except a few express vimentin (60, 61). As demonstrated by double labeling with anti-GFP and anti-vimentin, the results showed that Nes-S did not form filaments in the vimentin-free SW13 cells and presented a dispersed pattern throughout the cytoplasm (Fig. 5, *A–C*). On the other hand, the majority of the Nes-S protein co-localized with the vimentin filament in the vimentin$^+$ SW13 cells, whereas a subset of Nes-S presented a dotted appearance alongside the IF network (Fig. 5, *D–I*).

To verify whether Nes-S co-assembles into filaments with another two DRG neuronal IF proteins, *i.e.* peripherin and NFH, we transfected pEGFP-NestS into N2a neuroblastoma cells. N2a cells express peripherin in undifferentiated state when cultured in serum-containing medium and produce both peripherin and NFH upon serum deprivation-induced differentiation (62). After transfection, these cells were cultured in serum-containing medium for 2 days and subjected to triple labeling immunofluorescence microscopy with anti-GFP, anti-NFH, and anti-peripherin. The results showed that when expressed at medium to low levels, Nes-S co-assembled with peripherin into IFs, whereas NFH-IR was not detected (supplemental Fig. S9, *A–D*). To examine the assembly of Nes-S with NFH/peripherin filaments, the transfected N2a cells were cultured in serum-deprived medium for another 7 days and triple-labeled with anti-GFP, anti-NFH, and anti-peripherin. The results showed that nascent NFH protein formed filaments together with peripherin, and Nes-S co-assembled with these NFH$^+$/peripherin$^+$ filaments (supplemental Fig. S9, *E–H*). Taken together, we did not observe any IFs assembled solely from Nes-S in SW13 cells, N2a cells, primarily cultivated DRG neurons, or DRG tissue sections.

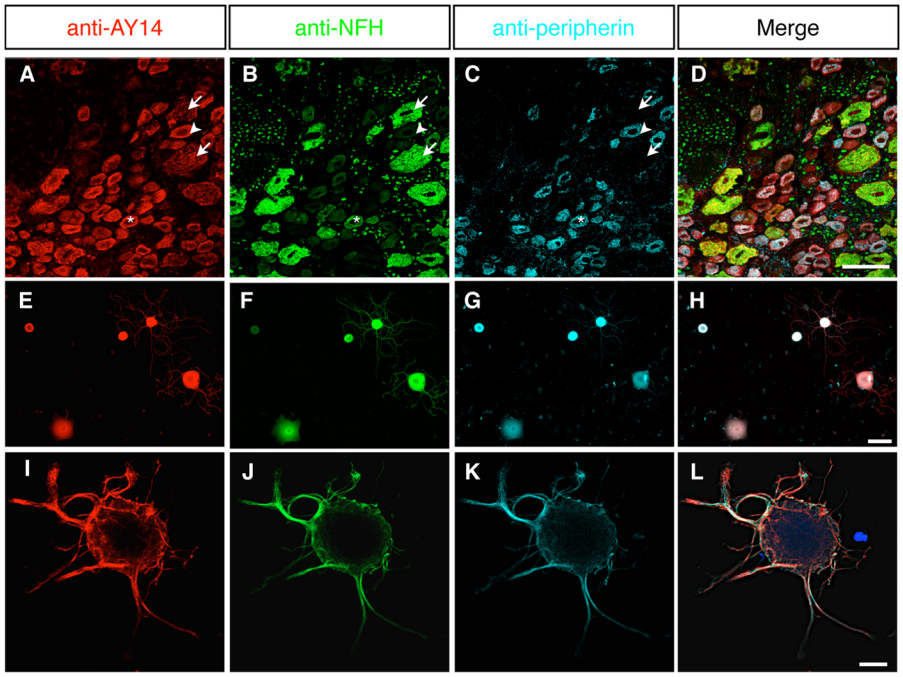

FIGURE 4. **Immunofluorescence localization of Nes-S protein in DRG neurons of adult rats.** *A–D*, triple labeling of DRG tissue sections of adult rats with anti-AY14 (*A*), anti-NFH (*B*), and anti-peripherin (*C*). All three populations of the DRG neurons, including NFH^+/$peripherin^-$ large neurons (*arrows*), NFH^+/$peripherin^+$ medium neurons (*asterisks*), and NFH^-/$peripherin^+$ small neurons (*arrowheads*), were $AY14^+$. *D* shows merged images. *Scale bar*: 50 μm. *E–H*, triple labeling of primary DRG neurons of adult rats with anti-AY14 (*E*), anti-NFH (*F*), and anti-peripherin (*G*). Anti-AY14-IR was observed in all of the neurons. *H* shows merged images. *Scale bar*: 50 μm. *I–L*, triple labeling of primary DRG neurons of adult rats with anti-AY14 (*I*), anti-NFH (*J*), and anti-peripherin (*K*) by high magnification confocal microscopy. The IFs formed a cage-like cytostructure at the periphery of neurons and extended into the neurites. *L* shows merged images. *Scale bar*: 15 μm.

Nes-S Expression during Postnatal DRG Development—To study the expression profile of Nes-S during the course of postnatal DRG development, IF-enriched preparation samples of DRG from rats of different postnatal days, starting from P0 to adult, were subjected to immunoblotting experiments with anti-AY14. The results revealed that Nes-S expression was not detected until P5, and its intensity increased at P8 and reached the highest point at adult (Fig. 6*A*). In addition, Nes-S was not detected in the Rat-401^+ neural stem cells, as shown by double labeling of cerebrum and spinal cord of the embryonic day 12 rat with anti-AY14 and Rat-401 (supplemental Fig. S10).

Tissue Distribution of Nes-S—To investigate the distribution of Nes-S in adult rats, IF-enriched preparations of various neural and muscle tissues, as well as other representative organs, *e.g.* heart, carotid artery, and kidney, were subjected to immunoblotting analysis with anti-AY14. The results showed that Nes-S was detected in DRG, trigeminal ganglia (TriG), superior cervical ganglia (SCG), and thoracic spinal cord (Fig. 6*B*). In addition, a trace amount of Nes-S was also detected in sciatic nerve (Fig. 6*B*).

To further examine the distribution pattern of Nes-S in nervous system, tissue sections of TriG, SCG, thoracic spinal cord, and sciatic nerve, as well as intestine, were subjected to triple labeling immunofluorescence microscopy with anti-AY14, anti-NFH, and anti-peripherin. The results revealed that all of the neurons in TriG and SCG presented anti-AY14-IR (Fig. 6, *C–J*). In the thoracic spinal cord, anti-AY14-IR was observed in the motor neurons at the ventral horn and preganglionic sympathetic neurons at the intermediate lateral region (Fig. 6, *K–R*). In sciatic nerve, a trace amount of anti-AY14-IR could be found in all of the axoplasm (Fig. 6, *S–V*). In the intestine, AY14-IR was only observed in the postsynaptic parasympathetic neurons (supplemental Fig. S11).

The Cytoprotective Effect of Nes-S in N2a Neuroblastoma Cells—Recent studies indicate that nestin exerts promitotic and prosurvival functions (4, 37, 41, 42). We first examined whether Nes-S promotes cell proliferation because differences in mitotic rate may interfere with the cell viability assay. N2a cells were transiently transfected with either pEGFP-NestS (N2a/NestS) or pEGFP plasmid (N2a/vector), and the protein expression was confirmed by immunoblotting with anti-GFP (supplemental Fig. S12*A*). These cells were cultured in either serum-containing or serum-free medium and subjected to MTT assay at various time points. Time-course MTT results revealed that in serum-containing medium, the growth rate of N2a/NestS cells was ~2-fold higher than that of N2a/vector cells (Fig. 7*A*). On the other hand, both cells of N2a/NestS and N2a/vector did not proliferate in serum-free medium (Fig. 7*A*). Thus, the subsequent cell viability assays were carried out using N2a cells cultured in serum-free medium.

To examine the effect of Nes-S on cell viability, N2a cells were transiently transfected with either pEGFP-NestS or pEGFP plasmid and subjected to limited dilutions. Three stable clones of both types of transfected cells were established. Immunofluorescence microscopy showed that all three N2a/NestS stable clones expressed Nes-S at medium to low levels. Subsequently, stable clones of N2a/NestS and N2a/vector, as well as untransfected N2a cells (N2a/wt), were cultured in serum-free medium for 12 h, treated with various concentrations of H_2O_2 for 24 h, and subjected to MTT assay. The results

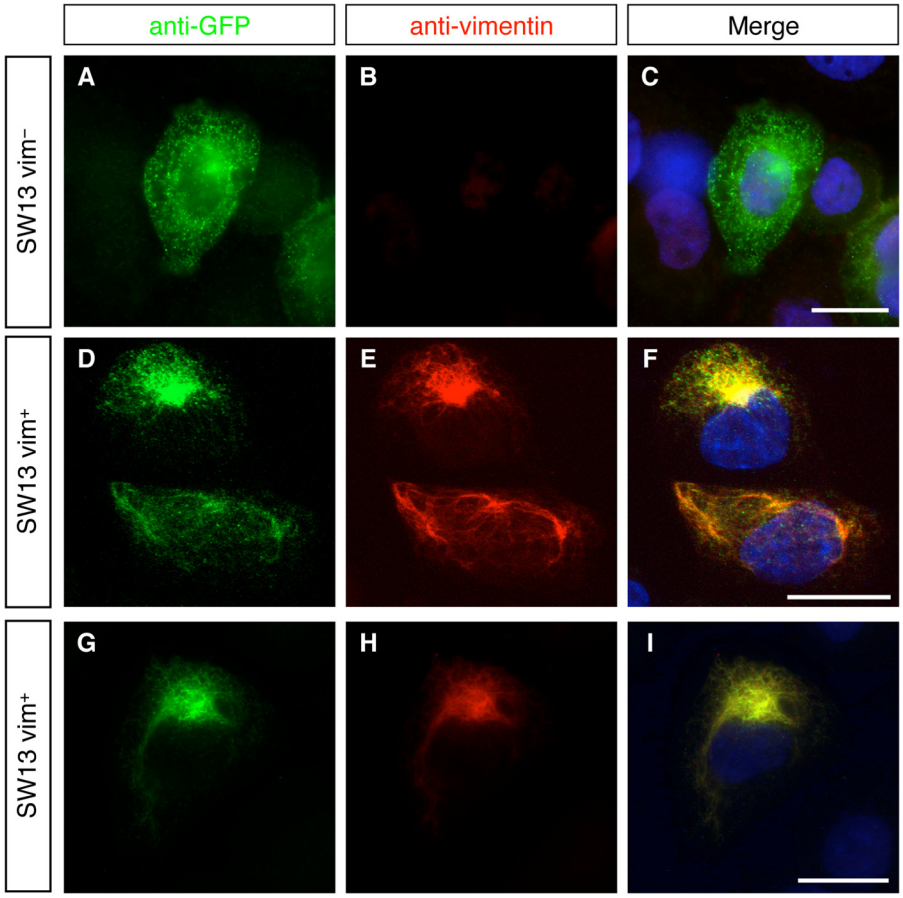

FIGURE 5. **Filament assembly properties of Nes-S.** *A–I*, double labeling of pEGFP-NestS-transfected SW13 cells with anti-GFP (*A*, *D*, and *G*) and anti-vimentin (*B*, *E*, and *H*). Nes-S presented a dispersed pattern in vimentin-free SW13 cells (*A–C*). The majority of the Nes-S protein co-localized with vimentin IF in the few SW13 cells that expressed vimentin (*D–I*). *Scale bar*: 15 μm.

showed that after treatments with 250 and 325 μM H_2O_2, the viability of all three N2a/NestS stable clones was significantly higher than that of N2a/vector and N2a/wt cells (Fig. 7*B*, also see supplemental Fig. S13*A*). In addition, transient transfection of Nes-S also rendered the cells more resistant to cell death (supplemental Fig. S12*B*). This result confirmed that this pro-survival effect was caused by Nes-S, but not by selecting for the stable cell clones. To verify whether the enhanced viability of N2a/NestS cells was due to inhibition of apoptotic pathways, we compared the time course of caspase-3 activation of N2a/NestS cells and N2a/vector cells under 250 μM H_2O_2 treatment. The results confirmed that expression of EGFP-tagged Nes-S attenuated the activation of caspase-3 (Fig. 7*C*). Taken together, the above observations indicate that Nes-S inhibits the H_2O_2-induced caspase-dependent apoptosis.

The Cdk5 phosphorylation site of nestin, Thr-316 (63), is retained in Nes-S. To investigate the interaction of endogenous Cdk5 with Nes-S, N2a cells transiently transfected with either pEGFP-NestS or pEGFP plasmid were subjected to co-immunoprecipitation assay. We were able to pull down Cdk5 with anti-GFP antibody from lysates of N2a/NestS cells, but not from that of N2a/vector cells (Fig. 7*D*). To examine whether the phosphorylation of Thr-316 affects the cytoprotective function of Nes-S, N2a cells were transfected with plasmids encoding either the T316A phospho-deficient mutant (N2a/NestS-T316A) or the T316D phospho-mimic mutant (N2a/NestS-T316D) of Nes-S. Subsequently, three stable clones of both types of transfected cells were established by limited dilutions. These clones were cultured in serum-free medium for 12 h, treated with 325 μM H_2O_2 for 24 h, and subjected to MTT assay. Stable clones of N2a/NestS and N2a/vector, as well as N2a/wt cells, were used as controls. The results showed that the viability of phospho-deficient N2a/NestS-T316A cells was significantly higher than that of N2a/NestS cells (Fig. 7*E*, also see supplemental Fig. S13*B*). In contrast, the viability of phospho-mimic N2a/NestS-T316D cells was significantly lower than that of N2a/NestS cells. No significant difference in viability was revealed among N2a/NestS-T316D, N2a/vector, and N2a/wt cells (Fig. 7*E*, also see supplemental Fig. S13*B*).

The Role of Nes-S in Survival of Primary DRG Neurons of Adult Rats—To study the cytoprotective effect of endogenous Nes-S, primary DRG neurons of adult rats were subjected to Nes-S RNAi knockdown experiments. The dissociated cells of DRG were transfected with either an shRNA expression plasmid that targets the rod domain of nestin or a noneffective shRNA expression plasmid as control. These two plasmids enable co-expression of shRNA and Turbo green fluorescent protein (tGFP) that serves as reporter to mark the transfected cells (Origene). To examine the transfection rate and the RNAi knockdown efficiency in DRG neurons, the transfected DRG cultures at the 7th day *in vitro* (DIV) were subjected to triple

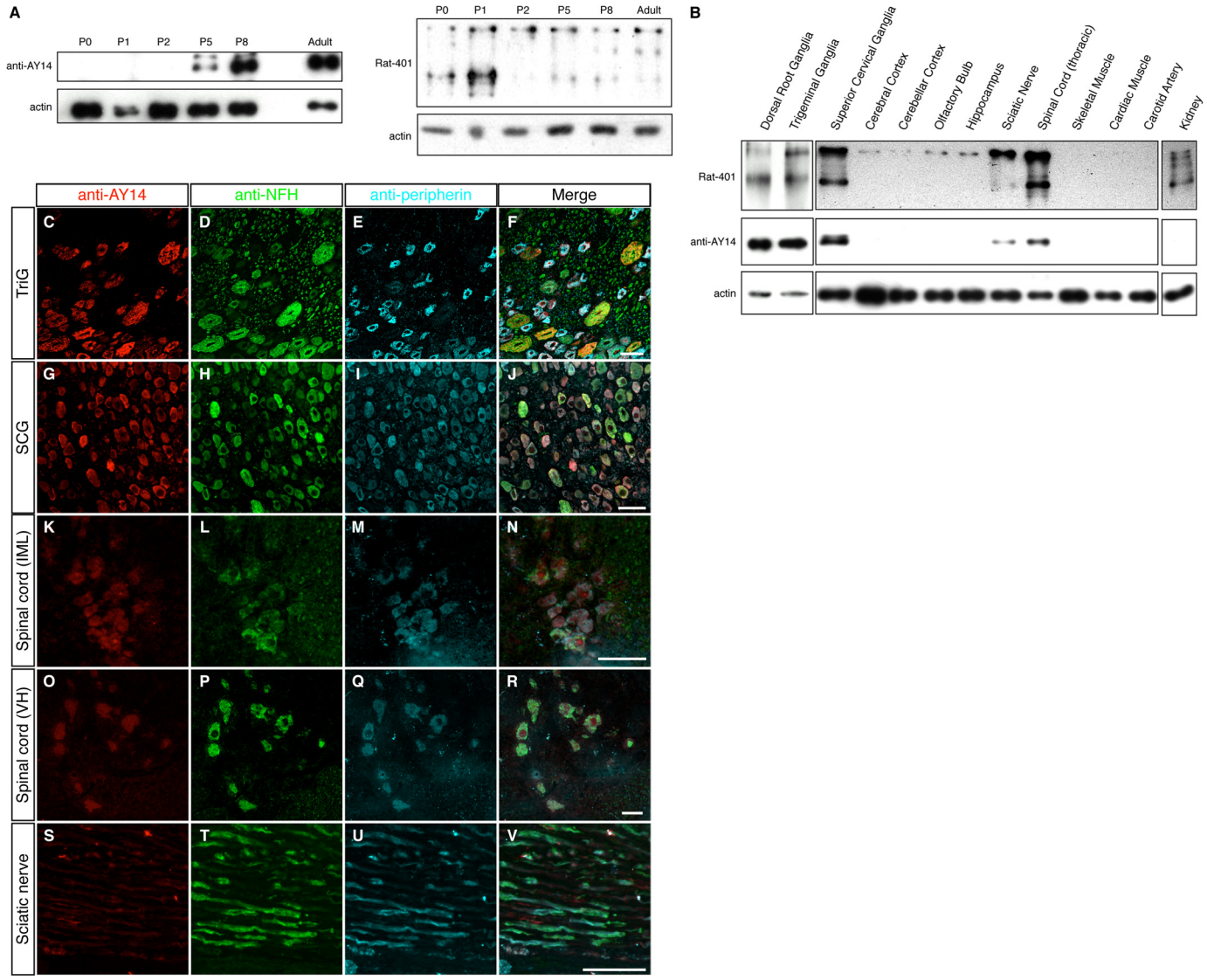

FIGURE 6. **Postnatal expression and tissue distribution of Nes-S.** *A*, immunoblotting of IF-enriched preparations of DRG from rats of different postnatal days, as well as the adult rats, with anti-AY14 and Rat-401. Nes-S expression was not detected until P5, and its intensity reached the highest point at adult. *B*, immunoblotting of IF-enriched preparations of various tissues of adult rats with anti-AY14 (*left*) and Rat-401 (*right*). Nes-S was expressed in DRG, TriG, SCG, and thoracic spinal cord, whereas a smaller amount of Nes-S was detected in sciatic nerve. *C–V*, triple labeling of TriG, SCG, spinal cord, and sciatic nerve of adult rats with anti-AY14, anti-NFH, and anti-peripherin. In TriG (*C–F*) and SCG (*G–J*), all neurons were $AY14^+$. In spinal cord, the preganglionic sympathetic neurons (*K–N*), and motor neurons (*O–R*) were $AY14^+$. In sciatic nerve, a trace amount of anti-AY14-IR was detected in the axoplasm of neurites (*S–V*). *IML*, intermediate lateral horn; *VH*, ventral horn. *Scale bar*: 50 μm.

labeling immunofluorescence microscopy with anti-AY14, anti-NFH, and anti-peripherin. The results showed that about 10% of neurons were $tGFP^+$ among all the DRG neurons in both groups. Furthermore, the anti-AY14-IR intensity decreased drastically in all $tGFP^+$ neurons that were transfected with nestin shRNA expression plasmid, whereas it remained the same in neurons transfected with control plasmid (Fig. 8, *A–H*). To examine the effect of Nes-S knockdown on the viability of DRG neurons, the numbers of $tGFP^+$ cells that presented a neuronal morphology were counted at 7, 11, and 15 DIV by time-course live cell imaging. The survival rate of each DIV was calculated using the number of $tGFP^+$ cells of the same plate at 7 DIV as the denominator. The results showed that the survival rate of Nes-S knockdown neurons (47.0 $\pm$ 1.8%) was significantly lower than that of noneffective control (70.9 $\pm$ 1.3%) at 11 DIV, indicating that Nes-S exerts a cytoprotective function in DRG neurons of adult rats (Fig. 8*I*, also see supplemental Table S2).

DISCUSSION

In the current study, we report the first isoform of nestin, Nes-S, in DRG neurons of adult rats. Nestin cannot form filaments by itself due to its short 7-aa N-terminal domain, which may not be sufficient to support stable assembly of nestin homopolymers (3, 21, 36). Instead, nestin forms heteropolymers with other IF proteins, such as the type III vimentin and the type IV α-internexin, but not with the type I/II keratin proteins (3, 36). The N-terminal domain and rod domain of Nes-S are identical to nestin. Nes-S cannot form filaments in the vimentin-free SW13 cells, and it is able to co-assemble into filaments with the type III vimentin and peripherin, as well as the type IV NFH. Taken together, these results indicated that

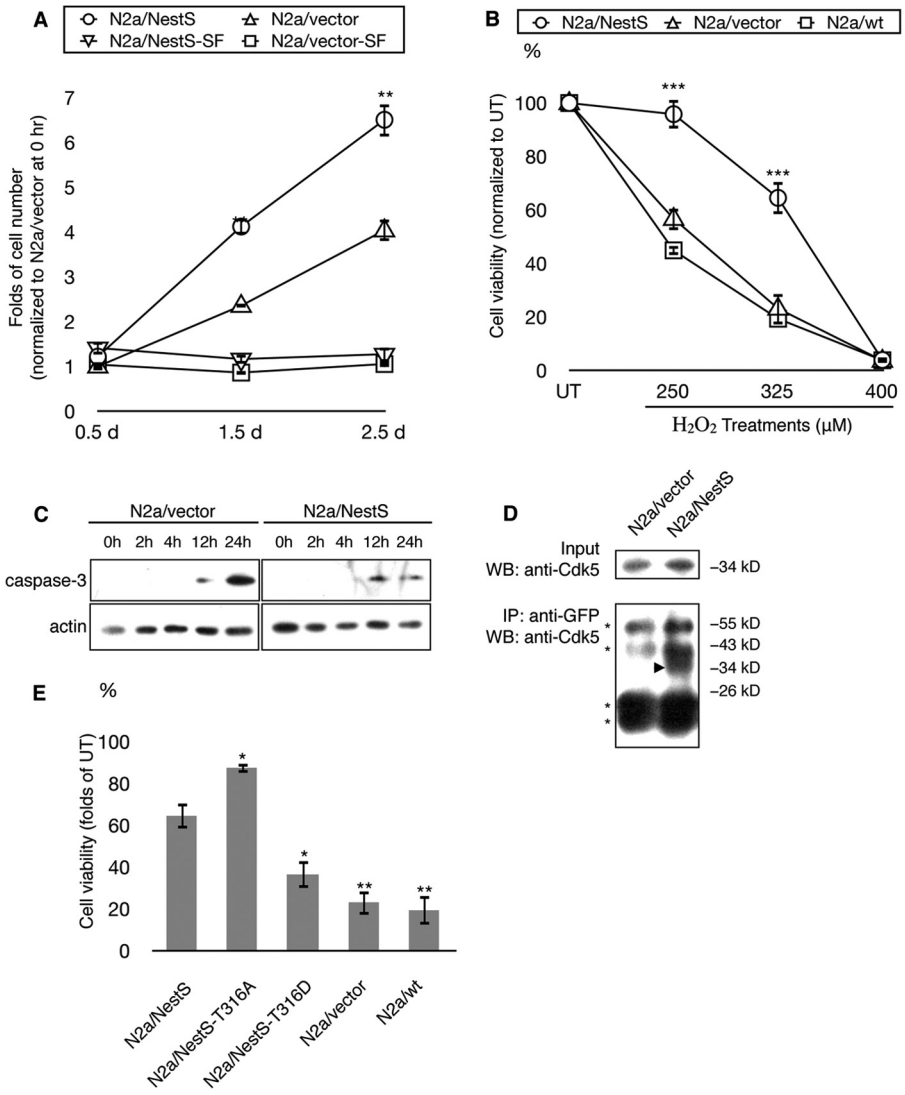

FIGURE 7. **The cytoprotective effect of Nes-S in N2a neuroblastoma cells.** *A*, promitotic function of Nes-S, as revealed by time-course MTT assays of N2a/NestS and N2a/vector cells. These cells were passaged 12 h before being cultured in either serum-containing (*S*) or serum-free (*SF*) medium. The time of medium change was designated as 0 h. The cell number at each time point was normalized to that of N2a/vector cells cultured in serum-containing medium at 0 h. The N2a/NestS cells showed an ~2-fold proliferation rate when cultured in serum-containing medium, as compared with N2a/vector cells ($n = 4$, **, $p < 0.01$, two-tailed *t* test). Both cell types did not proliferate in serum-free medium. *Error bars* indicate S.E. *B*, prosurvival function of Nes-S, as determined by MTT assays of N2a/NestS and N2a/vector cells, as well as untransfected N2a cells (*N2a/wt*). The survival rates of N2a/NestS cells upon 250 and 325 μM H_2O_2 treatments (95.8 ± 5.3 and 64.5 ± 6.0%, respectively) were significantly higher than those of N2a/vector cells (56.7 ± 4.2 and 23.2 ± 5.9%, respectively) and N2a/wt cells (44.9 ± 1.7 and 19.4 ± 6.8%, respectively). There was no significant difference in survival rates between N2a/vector cells and N2a/wt cells ($n = 4$, **, $p < 0.01$, ***, $p < 0.001$, two-tailed *t* test). *Error bars* indicate S.E. *C*, caspase-3 activation of N2a/NestS and N2a/vector cells. N2a cells transiently expressing either pEGFP (*N2a/vector*) or pEGFP-NestS (*N2a/NestS*) were subjected to serum starvation for 12 h and treated with 250 μM H_2O_2, and their whole cell extractions were collected at various time points. The results showed that expression of EGFP-tagged Nes-S protein attenuated the activation of caspase-3. *D*, co-immunoprecipitation of Cdk5 and EGFP-tagged Nes-S protein. N2a cells transiently expressing either pEGFP (*N2a/vector*) or pEGFP-NestS (*N2a/NestS*) were subjected to serum starvation for 24 h before harvesting. The lysates were immunoprecipitated with anti-GFP and immunoblotted (*WB*) with anti-Cdk5. Total lysates were also immunoblotted with anti-Cdk5 as a positive control. Cdk5 was detected in the immunoprecipitates (*IP*) from N2a/NestS lysates, but not in that from N2a/vector. *Arrowhead*, Cdk5. *Asterisks*, IgG bands. *E*, effect of Thr-316 point mutation on cytoprotective function of Nes-S. The viability of N2a/NestS-T316A cells was significantly higher than that of N2a/NestS cells (87.5 ± 2.3 and 64.5 ± 6.0%, respectively). The viability of N2a/NestS-T316D cells was significantly lower than that of N2a/NestS cells (36.5 ± 6.4 and 64.5 ± 6.0%, respectively). No significant difference in survival rates was observed among N2a/NestS-T316D, N2a/vector, and N2a/wt cells ($n = 4$, *, $p < 0.05$, **, $p < 0.01$, two-tailed *t* test). *Error bars* indicate S.E. *UT*, untreated.

Nes-S inherits the basic assembly properties of nestin. It is interesting to note that the sequences corresponding to the splicing junction of rat Nes-S, as well as its nearby sequences, are conserved among rat, mouse, and human, as revealed by multiple alignment analysis (supplemental Fig. S14). This observation implies that the existence of nestin isoform may be conserved across species.

Cdk5 signaling was shown to be involved in the functions of nestin (38, 39, 41, 42). In neuronal cells under normal conditions, Cdk5 is activated by binding to its co-activator p35, and the activated Cdk5 complex subsequently participates in various cellular processes, including neuron migration, neurite extension, synapse formation, and neuron survival (64, 65). However, in neuronal cells under stress, the activated Cdk5

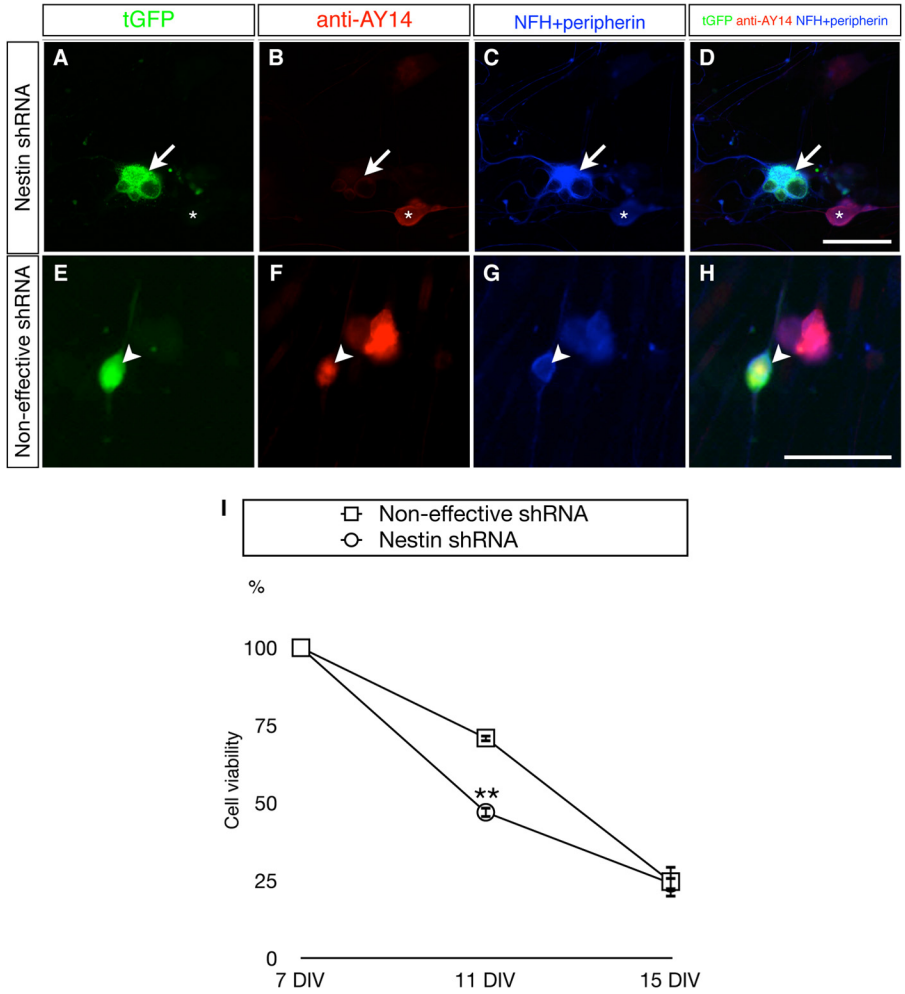

FIGURE 8. **Impaired cell survival in primary DRG neurons of adult rats upon RNAi knockdown of Nes-S.** *A–D*, reduced expression of Nes-S by nestin shRNA expression vector. The transfected neurons in the 7 DIV cultures were recognized by their tGFP expression (*A*) and morphological features, *i.e.* a rounded soma and elongated neurites. Triple labeling with anti-AY14 (*B*) and anti-NFH and anti-peripherin (*C*, their IRs were recorded in the same channel) showed that anti-AY14-IR intensity was reduced in DRG neurons expressing the tGFP reporter gene of shRNA vector (*arrow*). The anti-AY14-IR remained in the untransfected neurons (*asterisk*). *D* shows merged images. *E–H*, expression level of Nes-S was not altered by noneffective shRNA control vector. The $tGFP^+$ neurons (*E*, *arrowhead*) present AY14-IR (*F*) as well as NFH- and peripherin-IR (*G*). *H* shows merged images. *Scale bar*: 50 μm. *I*, reduced cell survival rate in Nes-S knockdown DRG neurons during prolonged culture. Live cell images of $tGFP^+$ neurons were taken by an inverted fluorescence microscope at 7, 11, and 15 DIV. At each day, the number of tGFP-expressing neurons was counted. The viability of Nes-S knockdown neurons was significantly decreased at 11 DIV ($n = 3$, **, $p < 0.01$, two-tailed *t* test). Neurons transfected with the noneffective shRNA vector were used as control. The survival rate of each DIV was calculated using the number of $tGFP^+$ cells of the same plate at 7 DIV as the denominator. For the number of neurons of both transfected groups at each day, see supplemental Table S2. *Error bars* indicate S.E.

complex is translocated into the nucleus and induces cell cycle re-entry, leading to p53-mediated apoptosis (64–69). Taken together, cytoplasmic Cdk5 activity exerts prosurvival effects, whereas nuclear Cdk5 activity is cytotoxic. Notably, the presence of nestin attenuates the intranuclear Cdk5-induced apoptosis. Sahlgren *et al.* (41) reported that nestin protects the ST15A neuroblastoma cells from H_2O_2-induced apoptosis by acting as a Cdk5-sequestering scaffold that retains Cdk5 within the cytoplasm and prevents its nuclear translocation. The cytoplasmic Cdk5 activity may in turn protect cells from apoptosis. Huang *et al.* (42) reported that in rat aortic smooth muscle cells under oxidative stress, nestin facilitates Cdk5-dependent Bcl-2 phosphorylation and subsequently prevents caspase-3 activation. Nestin is phosphorylated by Cdk5 at two threonine residues, Thr-316 and Thr-1495 (63). No functional study has been carried out on Thr-1495, which is removed in Nes-S. Previous studies indicated that in differentiating skeletal myocytes, Cdk5 binds to the unphosphorylated Thr-316 residue of nestin, which then facilitates Cdk5 activation by recruiting p35 (39, 63). The activated Cdk5 complex phosphorylates the Thr-316 residue and subsequently dissociates from the nestin scaffold (39, 63). In addition, it was demonstrated that the T316A phospho-deficient mutation of nestin markedly enhances its binding affinity to Cdk5, leading to a decrease in Cdk5 activity (39). It is of interest to note that in ST15A cells under oxidative stress, removal of a Thr-316-containing region of nestin abolished its cytoprotective effect (41). Therefore, binding of Cdk5 to the Thr-316 residue of nestin may increase the cytoplasm-to-nucleus ratio of Cdk5 activity and thus enhance cell survival. However, whether Thr-316 is responsible for the antiapoptotic function of nestin remains to be proven. In this study, our co-immunoprecipitation results demonstrated that endogenous Cdk5 binds to Nes-S in N2a cells. In addition, the cytoprotective effect of Nes-S was significantly enhanced by T316A phos-

pho-deficient mutation and was abolished by T316D phosphomimic mutation. It appears that the Cdk5-sequestering effect of Nes-S is improved upon T316A mutation and reduced upon T316D mutation. Taken together, our results confirmed that the Thr-316 residue is indispensable for the cytoprotective function of Nes-S. Our current study, together with the previous studies (41–44), suggests that nestin and Nes-S exert cytoprotective function by sequestering Cdk5 complex through the Thr-316 residue.

Recent studies on nestin knock-out mice showed two controversial results. One reported embryonic lethality and elevated levels of apoptosis of neural stem cells in nestin knock-out mice (70). In contrast, a more recent study of nestin knock-out mice from another research group did not show embryonic lethality, nor did it show any apparent morphological abnormalities in the CNS of adult mice (40). The major defect of these knock-out mice was the impaired motor coordination, as revealed by rotarod experiments. The muscle strength and body balance were not affected in these knock-out mice, whereas excess numbers of AChR clusters were observed in their neuromuscular junctions. Because the number of AChR clusters is regulated by nestin (39), the authors suggested that nestin knock-out leads to misregulated numbers of AChR clusters and contributes to impaired motor coordination. As to the former study (70), it is of interest to note that Nes-S is not involved in the embryonic lethality because it is expressed postnatally. As to the later study (40), given that Nes-S is expressed in both sensory and motor neurons of peripheral nervous system and exerts cytoprotective function, lack of Nes-S due to knock-out of nestin locus may also be one of the factors that affect the normal functions of somatosensory reflex circuits and result in the impaired dynamic motor coordination. However, the involvement of Nes-S in the impaired motor coordination is unclear and requires further in-depth investigations.

It is well known that during embryonic and perinatal development, DRG neurons undergo apoptosis when they fail to receive sufficient NGF secreted from their target tissues (57, 71–73). However, the neuronal survival becomes NGF-independent around P5, and this independency persists throughout adulthood (57, 74–76). In this study, our results showed that the expression of Nes-S first appeared in DRG neurons at P5. Given that Nes-S exerts a cytoprotective function, it may be involved in this NGF independency switch. Furthermore, our immunoblotting and immunofluorescence results revealed that the expression of Nes-S is restricted to the sensory and motor neurons, including sensory neurons of DRG and TriG and motor neurons of SCG and enteric plexus, as well as in motor neurons and preganglionic sympathetic neurons of thoracic spinal cord. The processes of these neurons extend toward the limbs or the periphery of the body and are susceptible to mechanical injuries. The expression of Nes-S may provide additional cytoprotection to support the long term survival of these motor and sensory neurons. One of the hallmarks of neurodegenerative diseases is the substantial neuronal death of the patients. The identification of Nes-S, which exerts a cytoprotective function in adult neurons, may shed light on future studies of neurodegenerative diseases.

Acknowledgments—We thank Drs. Chih-Tien Wang, Hsinyu Lee, Shyh-Jye Lee, Tsai-Kai Ju, Yuan-Li Huang, and Shau-Chi Chi for technical support. We also thank the Technology Commons, College of Life Science, National Taiwan University, for confocal microscopy equipment and Northern blotting.

REFERENCES

1. Lendahl, U., Zimmerman, L. B., and McKay, R. D. (1990) CNS stem cells express a new class of intermediate filament protein. *Cell* **60,** 585–595
2. Yang, H. Y., Lieska, N., Goldman, A. E., and Goldman, R. D. (1992) Colchicine-sensitive and colchicine-insensitive intermediate filament systems distinguished by a new intermediate filament-associated protein, IFAP-70/280 kD. *Cell Motil. Cytoskeleton* **22,** 185–199
3. Steinert, P. M., Chou, Y. H., Prahlad, V., Parry, D. A., Marekov, L. N., Wu, K. C., Jang, S. I., and Goldman, R. D. (1999) A high molecular weight intermediate filament-associated protein in BHK-21 cells is nestin, a type VI intermediate filament protein: limited co-assembly *in vitro* to form heteropolymers with type III vimentin and type IV α-internexin. *J. Biol. Chem.* **274,** 9881–9890
4. Chou, Y. H., Khuon, S., Herrmann, H., and Goldman, R. D. (2003) Nestin promotes the phosphorylation-dependent disassembly of vimentin intermediate filaments during mitosis. *Mol. Biol. Cell* **14,** 1468–1478
5. Guérette, D., Khan, P. A., Savard, P. E., and Vincent, M. (2007) Molecular evolution of type VI intermediate filament proteins. *BMC Evol. Biol.* **7,** 164
6. Chang, L., and Goldman, R. D. (2004) Intermediate filaments mediate cytoskeletal crosstalk. *Nat. Rev. Mol. Cell Biol.* **5,** 601–613
7. Herrmann, H., Bär, H., Kreplak, L., Strelkov, S. V., and Aebi, U. (2007) Intermediate filaments: from cell architecture to nanomechanics. *Nat. Rev. Mol. Cell Biol.* **8,** 562–573
8. Goldman, R. D., Cleland, M. M., Murthy, S. N. P., Mahammad, S., and Kuczmarski, E. R. (2012) Inroads into the structure and function of intermediate filament networks. *J. Struct. Biol.* **177,** 14–23
9. Yang, H. Y., Lieska, N., Goldman, A. E., and Goldman, R. D. (1985) A 300,000-mol-wt intermediate filament-associated protein in baby hamster kidney (BHK-21) cells. *J. Cell Biol.* **100,** 620–631
10. Herrmann, H., and Wiche, G. (1987) Plectin and IFAP-300K are homologous proteins binding to microtubule-associated proteins 1 and 2 and to the 240-kilodalton subunit of spectrin. *J. Biol. Chem.* **262,** 1320–1325
11. Karakesisoglou, I., Yang, Y., and Fuchs, E. (2000) An epidermal plakin that integrates actin and microtubule networks at cellular junctions. *J. Cell Biol.* **149,** 195–208
12. Leung, C. L., Liem, R. K., Parry, D. A., and Green, K. J. (2001) The plakin family. *J. Cell Sci.* **114,** 3409–3410
13. Leung, C. L., Green, K. J., and Liem, R. K. H. (2002) Plakins: a family of versatile cytolinker proteins. *Trends Cell Biol.* **12,** 37–45
14. Wu, X., Kodama, A., and Fuchs, E. (2008) ACF7 regulates cytoskeletal-focal adhesion dynamics and migration and has ATPase activity. *Cell* **135,** 137–148
15. Goldman, R. D., and Steinert, P. M. (1990) *Cellular and Molecular Biology of Intermediate Filaments*, pp. 3–17, Plenum Publishing Corp., New York
16. Parry, D. A. D. (2005) Microdissection of the sequence and structure of intermediate filament chains. *Adv. Protein Chem.* **70,** 113–142
17. Omary, M. B., Ku, N. O., Tao, G. Z., Toivola, D. M., and Liao, J. (2006) "Heads and tails" of intermediate filament phosphorylation: multiple sites and functional insights. *Trends. Biochem. Sci.* **31,** 383–394
18. Parry, D. A., Strelkov, S. V., Burkhard, P., Aebi, U., and Herrmann, H. (2007) Towards a molecular description of intermediate filament structure and assembly. *Exp. Cell Res.* **313,** 2204–2216
19. Herrmann, H., and Aebi, U. (2000) Intermediate filaments and their associates: multi-talented structural elements specifying cytoarchitecture and cytodynamics. *Curr. Opin. Cell Biol.* **12,** 79–90
20. Granger, B. L., and Lazarides, E. (1980) Synemin: a new high molecular weight protein associated with desmin and vimentin filaments in muscle.

Cell **22,** 727–738
21. Michalczyk, K., and Ziman, M. (2005) Nestin structure and predicted function in cellular cytoskeletal organisation. *Histol. Histopathol.* **20,** 665–671
22. Dahlstrand, J., Zimmerman, L. B., McKay, R. D., and Lendahl, U. (1992) Characterization of the human nestin gene reveals a close evolutionary relationship to neurofilaments. *J. Cell Sci.* **103,** 589–597
23. Wiese, C., Rolletschek, A., Kania, G., Blyszczuk, P., Tarasov, K. V., Tarasova, Y., Wersto, R. P., Boheler, K. R., and Wobus, A. M. (2004) Nestin expression–a property of multi-lineage progenitor cells? *Cell Mol. Life Sci.* **61,** 2510–2522
24. Hyder, C. L., Isoniemi, K. O., Torvaldson, E. S., and Eriksson, J. E. (2011) Insights into intermediate filament regulation from development to ageing. *J. Cell Sci.* **124,** 1363–1372
25. Zimmerman, L., Parr, B., Lendahl, U., Cunningham, M., McKay, R., Gavin, B., Mann, J., Vassileva, G., and McMahon, A. (1994) Independent regulatory elements in the nestin gene direct transgene expression to neural stem cells or muscle precursors. *Neuron* **12,** 11–24
26. Tanaka, S., Kamachi, Y., Tanouchi, A., Hamada, H., Jing, N., and Kondoh, H. (2004) Interplay of SOX and POU factors in regulation of the Nestin gene in neural primordial cells. *Mol. Cell. Biol.* **24,** 8834–8846
27. Jin, Z., Liu, L., Bian, W., Chen, Y., Xu, G., Cheng, L., and Jing, N. (2009) Different transcription factors regulate nestin gene expression during P19 cell neural differentiation and central nervous system development. *J. Biol. Chem.* **284,** 8160–8173
28. Huang, Y. L., Shi, G. Y., Jiang, M. J., Lee, H., Chou, Y. W., Wu, H. L., and Yang, H. Y. (2008) Epidermal growth factor up-regulates the expression of nestin through the Ras-Raf-ERK signaling axis in rat vascular smooth muscle cells. *Biochem. Biophys. Res. Commun.* **377,** 361–366
29. Oikawa, H., Hayashi, K., Maesawa, C., Masuda, T., and Sobue, K. (2010) Expression profiles of nestin in vascular smooth muscle cells *in vivo* and *in vitro*. *Exp. Cell Res.* **316,** 940–950
30. Hockfield, S., and McKay, R. D. (1985) Identification of major cell classes in the developing mammalian nervous system. *J. Neurosci.* **5,** 3310–3328
31. Yang, H. Y., Lieska, N., Shao, D., Kriho, V., and Pappas, G. D. (1993) Immunotyping of radial glia and their glial derivatives during development of the rat spinal cord. *J. Neurocytol.* **22,** 558–571
32. Hendrickson, M. L., Rao, A. J., Demerdash, O. N. A., and Kalil, R. E. (2011) Expression of nestin by neural cells in the adult rat and human brain. *PLoS ONE* **6,** e18535
33. Frisén, J., Johansson, C. B., Török, C., Risling, M., and Lendahl, U. (1995) Rapid, widespread, and longlasting induction of nestin contributes to the generation of glial scar tissue after CNS injury. *J. Cell Biol.* **131,** 453–464
34. Yang, H. Y., Lieska, N., Kriho, V., Wu, C. M., and Pappas, G. D. (1997) A subpopulation of reactive astrocytes at the immediate site of cerebral cortical injury. *Exp. Neurol.* **146,** 199–205
35. Lee, C. Y., Pappas, G. D., Kriho, V., Huang, B. M., and Yang, H. Y. (2003) Proliferation of a subpopulation of reactive astrocytes following needle-insertion lesion in rat. *Neurol. Res.* **25,** 767–776
36. Marvin, M. J., Dahlstrand, J., Lendahl, U., and McKay, R. D. (1998) A rod end deletion in the intermediate filament protein nestin alters its subcellular localization in neuroepithelial cells of transgenic mice. *J. Cell Sci.* **111,** 1951–1961
37. Huang, Y. L., Shi, G. Y., Lee, H., Jiang, M. J., Huang, B. M., Wu, H. L., and Yang, H. Y, (2009) Thrombin induces nestin expression via the transactivation of EGFR signalings in rat vascular smooth muscle cells. *Cell Signal* **21,** 954–968
38. Pallari, H. M., Lindqvist, J., Torvaldson, E., Ferraris, S. E., He, T., Sahlgren, C., and Eriksson, J. E. (2011) Nestin as a regulator of Cdk5 in differentiating myoblasts. *Mol. Biol. Cell* **22,** 1539–1549
39. Yang, J., Dominguez, B., de Winter, F., Gould, T. W., Eriksson, J. E., and Lee, K. F. (2011) Nestin negatively regulates postsynaptic differentiation of the neuromuscular synapse. *Nat. Neurosci.* **14,** 324–330
40. Mohseni, P., Sung, H.-K., Murphy, A. J., Laliberte, C. L., Pallari, H. M., Henkelman, M., Georgiou, J., Xie, G., Quaggin, S. E., Thorner, P. S., Eriksson, J. E., and Nagy, A. (2011) Nestin is not essential for development of the CNS but required for dispersion of acetylcholine receptor clusters at the area of neuromuscular junctions. *J. Neurosci.* **31,** 11547–11552
41. Sahlgren, C. M., Pallari, H. M., He, T., Chou, Y. H., Goldman, R. D., and Eriksson, J. E. (2006) A nestin scaffold links Cdk5/p35 signaling to oxidant-induced cell death. *EMBO J.* **25,** 4808–4819
42. Huang, Y. L., Wu, C. M., Shi, G. Y., Wu, G. C. C., Lee, H., Jiang, M. J., Wu, H. L., and Yang, H. Y. (2009) Nestin serves as a prosurvival determinant that is linked to the cytoprotective effect of epidermal growth factor in rat vascular smooth muscle cells. *J. Biochem.* **146,** 307–315
43. Toivola, D. M., Strnad, P., Habtezion, A., and Omary, M. B. (2010) Intermediate filaments take the heat as stress proteins. *Trends Cell Biol.* **20,** 79–91
44. Liu, W., Zhang, Y., Hao, J., Liu, S., Liu, Q., Zhao, S., Shi, Y., and Duan, H. (2012) Nestin protects mouse podocytes against high glucose-induced apoptosis by a Cdk5-dependent mechanism. *J. Cell. Biochem.* **113,** 3186–3196
45. Park, K. Y., Dalakas, M. C., Goebel, H. H., Ferrans, V. J., Semino-Mora, C., Litvak, S., Takeda, K., and Goldfarb, L. G. (2000) Desmin splice variants causing cardiac and skeletal myopathy. *J. Med. Genet.* **37,** 851–857
46. Xue, Z. G., Cheraud, Y., Brocheriou, V., Izmiryan, A., Titeux, M., Paulin, D., and Li, Z. (2004) The mouse synemin gene encodes three intermediate filament proteins generated by alternative exon usage and different open reading frames. *Exp. Cell Res.* **298,** 431–444
47. Blechingberg, J., Holm, I. E., Nielsen, K. B., Jensen, T. H., Jørgensen, A. L., and Nielsen, A. L. (2007) Identification and characterization of GFAPκ, a novel glial fibrillary acidic protein isoform. *Glia* **55,** 497–507
48. McLean, J., Xiao, S., Miyazaki, K., and Robertson, J. (2008) A novel peripherin isoform generated by alternative translation is required for normal filament network formation. *J. Neurochem.* **104,** 1663–1673
49. Perng, M. D., Wen, S. F., Gibbon, T., Middeldorp, J., Sluijs, J., Hol, E. M., and Quinlan, R. A. (2008) Glial fibrillary acidic protein filaments can tolerate the incorporation of assembly-compromised GFAP-δ, but with consequences for filament organization and αB-crystallin association. *Mol. Biol. Cell* **19,** 4521–4533
50. Xiao, S., Tjostheim, S., Sanelli, T., McLean, J. R., Horne, P., Fan, Y., Ravits, J., Strong, M. J., and Robertson, J. (2008) An aggregate-inducing peripherin isoform generated through intron retention is upregulated in amyotrophic lateral sclerosis and associated with disease pathology. *J. Neurosci.* **28,** 1833–1840
51. Langbein, L., Eckhart, L., Rogers, M. A., Praetzel-Wunder, S., and Schweizer, J. (2010) Against the rules: human keratin K80: two functional alternative splice variants, K80 and K80.1, with special cellular localization in a wide range of epithelia. *J. Biol. Chem.* **285,** 36909–36921
52. Zhou, Z., Kahns, S., and Nielsen, A. L. (2010) Identification of a novel vimentin promoter and mRNA isoform. *Mol. Biol. Rep.* **37,** 2407–2413
53. Yuan, Y., Lee, J. A., Napier, A., and Cole, G. J. (1997) Molecular cloning of a new intermediate filament protein expressed by radial glia and demonstration of alternative splicing in a novel heptad repeat region located in the carboxy-terminal tail domain. *Mol. Cell. Neurosci.* **10,** 71–86
54. Izmiryan, A., Cheraud, Y., Khanamiryan, L., Leterrier, J. F., Federici, T., Peltekian, E., Moura-Neto, V., Paulin, D., Li, Z., and Xue, Z. G. (2006) Different expression of synemin isoforms in glia and neurons during nervous system development. *Glia* **54,** 204–213
55. Izmiryan, A., Franco, C. A., Paulin, D., Li, Z., and Xue, Z. (2009) Synemin isoforms during mouse development: multiplicity of partners in vascular and neuronal systems. *Exp. Cell Res.* **315,** 769–783
56. Su, P. H., Wang, T. C., Wong, Z. R., Huang, B. M., and Yang, H. Y. (2011) The expression of nestin delineates skeletal muscle differentiation in the developing rat esophagus. *J. Anat.* **218,** 311–323
57. Lindsay, R. M. (1988) Nerve growth factors (NGF, BDNF) enhance axonal regeneration but are not required for survival of adult sensory neurons. *J. Neurosci.* **8,** 2394–2405
58. Friedman, B., Zaremba, S., and Hockfield, S. (1990) Monoclonal antibody rat 401 recognizes Schwann cells in mature and developing peripheral nerve. *J. Comp. Neurol.* **295,** 43–51
59. Ferri, G. L., Sabani, A., Abelli, L., Polak, J. M., Dahl, D., and Portier, M. M. (1990) Neuronal intermediate filaments in rat dorsal root ganglia: differential distribution of peripherin and neurofilament protein immunoreactivity and effect of capsaicin. *Brain Res.* **515,** 331–335
60. Hedberg, K. K., and Chen, L. B. (1986) Absence of intermediate filaments

in a human adrenal cortex carcinoma-derived cell line. *Exp. Cell Res.* **163,** 509–517
61. Sarria, A. J., Nordeen, S. K., and Evans, R. M. (1990) Regulated expression of vimentin cDNA in cells in the presence and absence of a preexisting vimentin filament network. *J. Cell Biol.* **111,** 553–565
62. De Girolamo, L. A., Billett, E. E., and Hargreaves, A. J. (2000) Effects of 1-methyl-4-phenyl-1,2,3,6-tetrahydropyridine on differentiating mouse N2a neuroblastoma cells. *J. Neurochem.* **75,** 133–140
63. Sahlgren, C. M., Mikhailov, A., Vaittinen, S., Pallari, H.-M., Kalimo, H., Pant, H. C., and Eriksson, J. E. (2003) Cdk5 regulates the organization of Nestin and its association with p35. *Mol. Cell. Biol.* **23,** 5090–5106
64. Dhavan, R., and Tsai, L. H. (2001) A decade of CDK5. *Nat. Rev. Mol. Cell Biol.* **2,** 749–759
65. O'Hare, M. J., Kushwaha, N., Zhang, Y., Aleyasin, H., Callaghan, S. M., Slack, R. S., Albert, P. R., Vincent, I., and Park, D. S. (2005) Differential roles of nuclear and cytoplasmic cyclin-dependent kinase 5 in apoptotic and excitotoxic neuronal death. *J. Neurosci.* **25,** 8954–8966
66. Lee, J.-H., Kim, H.-S., Lee, S.-J., and Kim, K.-T. (2007) Stabilization and activation of p53 induced by Cdk5 contributes to neuronal cell death. *J. Cell Sci.* **120,** 2259–2271
67. Saito, T., Konno, T., Hosokawa, T., Asada, A., Ishiguro, K., and Hisanaga, S.-I. (2007) p25/Cyclin-dependent kinase 5 promotes the progression of cell death in nucleus of endoplasmic reticulum-stressed neurons. *J. Neurochem.* **102,** 133–140
68. Lopes, J. P., Oliveira, C. R., and Agostinho, P. (2009) Cdk5 acts as a mediator of neuronal cell cycle re-entry triggered by amyloid-β and prion peptides. *Cell Cycle* **8,** 97–104
69. Tian, B., Yang, Q., and Mao, Z. (2009) Phosphorylation of ATM by Cdk5 mediates DNA damage signalling and regulates neuronal death. *Nat. Cell Biol.* **11,** 211–218
70. Park, D., Xiang, A. P., Mao, F. F., Zhang, L., Di, C.-G., Liu, X.-M., Shao, Y., Ma, B.-F., Lee, J.-H., Ha, K.-S., Walton, N., and Lahn, B. T. (2010) Nestin is required for the proper self-renewal of neural stem cells. *Stem Cells* **28,** 2162–2171
71. Pearson, J., Johnson, E. M., and Brandeis, L. (1983) Effects of antibodies to nerve growth factor on intrauterine development of derivatives of cranial neural crest and placode in the guinea pig. *Dev. Biol.* **96,** 32–36
72. Johnson, E., Jr., and Rich, K. (1986) The role of NGF in sensory neurons *in vivo*. *Trends Neurosci.* **9,** 33–37
73. Oppenheim, R. W. (1991) Cell death during development of the nervous system. *Annu. Rev. Neurosci.* **14,** 453–501
74. Tong, J. X., Eichler, M. E., and Rich, K. M. (1996) Intracellular calcium levels influence apoptosis in mature sensory neurons after trophic factor deprivation. *Exp. Neurol.* **138,** 45–52
75. Vogelbaum, M. A., Tong, J. X., and Rich, K. M. (1998) Developmental regulation of apoptosis in dorsal root ganglion neurons. *J. Neurosci.* **18,** 8928–8935
76. Ernsberger, U. (2009) Role of neurotrophin signalling in the differentiation of neurons from dorsal root ganglia and sympathetic ganglia. *Cell Tissue Res.* **336,** 349–384